

Quantum oscillation signatures of the Bloch-Grüneisen temperature in the Dirac semimetal ZrTe₅

S. Galeski^{1,2}, K. Araki,³ O. K. Forslund,^{4,5} R. Wawrzyńczak,⁶ H. F. Legg,⁷ P. K. Sivakumar,⁸ U. Miniotaite,⁹ F. Elson,⁹ M. Månsson,⁹ C. Witteveen,¹⁰ F. O. von Rohr,¹⁰ A. Q. R. Baron,¹¹ D. Ishikawa,¹¹ Q. Li,¹² G. Gu,¹² L. X. Zhao,^{13,14,15} W. L. Zhu,^{13,15,16} G. F. Chen,^{13,14,15} Y. Wang,¹³ S. S. P. Parkin,⁸ D. Grobunov,² S. Zherlitsyn,² B. Vlaar,¹⁷ D. H. Nguyen,¹⁷ S. Paschen,¹⁷ P. Narang,¹⁸ C. Felser,⁷ J. Wosnitza,^{19,20} T. Meng,²¹ Y. Sassa,²² S. A. Hartnoll,²³ and J. Gooth^{1,6}

¹Physikalisches Institut, *Universität Bonn*, Nussallee 12, 53115 Bonn, Germany

²Hochfeld-Magnetlabor Dresden (HLD-EMFL) and Würzburg-Dresden Cluster of Excellence ct.qmat, *Helmholtz-Zentrum Dresden-Rossendorf*, 01328 Dresden, Germany

³Applied Physics, *National Defense Academy*, Yokosuka, Kanagawa 239-8686, Japan

⁴Physik-Institut, *Universität Zurich*, Winterthurerstrasse 190, CH-8057 Zurich, Switzerland

⁵Department of Physics and Astronomy, *Uppsala University*, Box 516, SE-75120 Uppsala, Sweden

⁶Max Planck Institute for Chemical Physics of Solids, Nothnitzer Straße 40, 01187 Dresden, Germany

⁷Department of Physics, *University of Basel*, Klingelbergstrasse 82, CH-4056 Basel, Switzerland

⁸Max Planck Institute of Microstructure Physics, Weinberg 2, 06120 Halle (Saale), Germany

⁹Department of Applied Physics, *KTH Royal Institute of Technology*, SE-106 91 Stockholm, Sweden

¹⁰Department of Quantum Matter Physics, *University of Geneva*, Quai Ernest-Ansermet 24, 1211 Geneva, Switzerland

¹¹Precision Spectroscopy Division, CSRR, SPring-8/JASRI, Sayo, Hyogo 679-5198, Japan

¹²Condensed Matter Physics and Materials Science Department, *Brookhaven National Laboratory*, Upton, New York, USA

¹³Beijing National Laboratory for Condensed Matter Physics, *Institute of Physics, Chinese Academy of Sciences*, Beijing 100190, China

¹⁴Songshan Lake Materials Laboratory, Dongguan, Guangdong 523808, China

¹⁵School of Physics Science, *University of Chinese Academy of Sciences*, Beijing 100049, China

¹⁶School of Physics and Information Technology, *Shaanxi Normal University*, Xi'an 710062, China

¹⁷Institute of Solid State Physics, *TU Wien*, Wiedner Hauptstr. 8-10, 1040 Vienna, Austria

¹⁸College of Letters and Science, *University of California, Los Angeles*, California 90095, USA

¹⁹Institut für Festkörper- und Materialphysik, *Technische Universität Dresden*,

01069 Dresden, Germany

²⁰Institute of Theoretical Physics and Würzburg-Dresden Cluster of Excellence ct.qmat,

Technische Universität Dresden, 01069 Dresden, Germany

²¹Institute of Theoretical Physics and Würzburg-Dresden Cluster of Excellence ct.qmat,

Technische Universität Dresden, 01062 Dresden, Germany

²²Department of Physics, *Chalmers University of Technology*, Kemigården 1, 412 96 Gothenburg, Sweden

²³Department of Applied Mathematics and Theoretical Physics, *University of Cambridge*, Cambridge CB3 0WA, United Kingdom



(Received 14 December 2023; revised 10 April 2024; accepted 8 August 2024; published 10 September 2024)

The electron-phonon interaction is in many ways a solid state equivalent of quantum electrodynamics. Being always present, the e-p coupling is responsible for the intrinsic resistance of metals at finite temperatures, making it one of the most fundamental interactions present in solids. In typical metals, different regimes of e-p scattering are separated by a characteristic phonon energy scale—the Debye temperature. However, in metals harboring very small Fermi surfaces a new scale emerges—the Bloch-Grüneisen temperature. This is a temperature at which the average phonon momentum becomes comparable to the Fermi momentum of the electrons. Here we report sub-Kelvin transport and sound propagation experiments on the Dirac semimetal ZrTe₅. The combination of the simple band structure with only a single small Fermi surface sheet allowed us to directly observe the Bloch-Grüneisen temperature and its consequences on electronic transport of a 3D metal in the limit where the small size of the Fermi surface leads to effective restoration of translational invariance of free space. Our results indicate that on entering this hydrodynamic transport regime, the viscosity of the Dirac electronic liquid undergoes an anomalous increase beyond the theoretically predicted T^5 temperature dependence. Extension of our measurements to strong magnetic fields reveal that, despite the dimensional reduction of the electronic band structure, the electronic liquid retains characteristics of the zero-field hydrodynamic regime up to the quantum limit. This is vividly reflected by an anomalous suppression of the amplitude of quantum oscillations seen in the Shubnikov-de Haas effect.

DOI: [10.1103/PhysRevB.110.L121103](https://doi.org/10.1103/PhysRevB.110.L121103)

The ability to conduct electrical current is one of the most basic characteristics of metals. In simple materials, where

resistance is dominated by scattering of charge carriers by lattice vibrations, the temperature dependence of resistance falls

into two regimes [1,2]: At high temperatures above the Debye Temperature Θ_D , dynamics of the lattice can be described as an ensemble of independent classical oscillators, giving rise to electron scattering rate that is linear in temperature. In contrast, at low temperature, below Θ_D , intrinsic resistance emerges from scattering of charge carriers with bosonic quasiparticles that represent the collective excitations of the lattice—phonons. At low temperature, only acoustic phonons with momentum $k_{ph} = (k_B T)/(\hbar v_s)$ smaller than the Debye sphere (k_D), where v_s is the speed of sound, are populated and can take part in scattering, leading to a much stronger temperature dependence of resistance $R(T) \propto T^5$. The situation, however, is different in materials hosting small Fermi surfaces (FS) such as semimetals [3,4]. In electron-phonon (e-p) collisions, the maximum allowed phonon scattering momentum is limited to $2k_F$ —twice the Fermi wave vector. This leads to a new temperature scale—the Bloch-Grüneisen temperature $\Theta_{BG} = 2\hbar v_s k_F / k_B$, below which phonon scattering can no longer access the entire Fermi surface phase space, marking the crossover between T^5 and T -linear resistance. Furthermore, it has been predicted that cooling below Θ_{BG} can lead to appearance of a range of novel phenomena including increase of the electron liquid viscosity and increase of the effective electron mass due to e-p interactions [5,6].

In this work we describe sub-Kelvin charge transport and ultrasound propagation measurements on the Dirac semimetal ZrTe₅. Our results indicate an unconventional increase of electron viscosity on crossing Θ_{BG} , adding to the previously reported observation of phonon hydrodynamics observed in thermal transport [7]. Furthermore, magnetoresistance measurements reveal an anomalous suppression of the Shubnikov-de Haas effect at sub-Kelvin temperatures. Additional analysis of magnetoacoustics quantum oscillations (QO) and magnetoresistance in samples containing single and multiple FS sheets indicates that the anomalous behavior of SdH amplitudes is likely an electronic effect related to the suppression of Umklapp process and decoupling of the electron liquid from the lattice in low-density samples. It is interesting to note that a somewhat similar anomaly of the SdH oscillations has been reported in SmSb, where it has been attributed to emergent surface states in an antiferromagnetic phase [8,9].

The pentatelluride material family (ZrTe₅ and HfTe₅) has risen to prominence in recent years as an excellent solid-state realization of the 3D Dirac Hamiltonian and material candidates to harbor a topological insulating ground state [10,11]. Recent studies showed that, due to the exceptional purity [electron mobilities $\mu_e \approx 200\,000\text{ cm}^2/(\text{Vs})$] most properties, down to $T = 2\text{ K}$, can be well accounted for using a simple low energy description [12,13] making both ZrTe₅ and HfTe₅ [14–16] one of the best understood Dirac systems. ZrTe₅ is a diamagnetic metal and shows no signatures of magnetic interactions. While it has been shown to undergo a Lifshitz transition in the range of $T_L = 70 - 130\text{ K}$ [17–19], inducing a change in charge-carrier type, at low temperatures it is believed to be a simple metal.

Despite this apparent simplicity, the Fermi surface of the pentatellurides sensitively depends on the location of the chemical potential. Samples with small charge carrier density are characterized by a single elliptical electronlike Fermi

surface at the Gamma point covering only a few percent of the Brillouin zone (BZ). Such small FS together with the low sound velocity of acoustic phonons provide an ideal setting for studying the crossover between different phonon scattering regimes [12] with the estimated Θ_{BG} of only a few K. In contrast, in samples with a slightly higher charge carrier density, the chemical potential crosses additional bands giving rise to additional Fermi surface sheets in the corners of the BZ [19,20]. The additional scattering channels available in those samples provide a reference where physics related to the low Θ_{BG} temperature should be suppressed.

Here, we studied ZrTe₅ samples with different charge carrier densities to sub-Kelvin temperatures and examined their electrical transport in quantizing magnetic fields. For clarity of presentation in the remainder of the manuscript we primarily display data measured on two samples (A and B), differing in carrier density, with data on additional samples presented in the Supplemental Material. In all samples, the four-terminal longitudinal electrical resistivity ρ_{xx} and the Hall resistivity ρ_{xy} were measured with the electrical current applied along the crystallographic a axis and the magnetic field \mathbf{B} applied along the b axis; low field Hall effect measurements were used to extract the sample charge carrier densities, for details see the Supplemental Material [21].

Results of magnetoresistance measurements on samples A and B are shown in Figs. 1(a) and 1(b). Both samples display pronounced Shubnikov de-Haas oscillations exhibiting, however, very different frequencies. The oscillations frequencies, Figs. 1(c) and 1(d), and charge carrier density extracted from Hall measurements (for details see the SM) are in good agreement with the established band structure of ZrTe₅: increasing electron filling leads to expansion of the central Dirac FS and appearance of an additional oscillation frequency—reflecting that the chemical potential increases past the bottom of an additional quadratic band located at the R point in the BZ, for details see the SM.

Investigation of the temperature dependence of the SdH oscillations amplitudes reveals an intriguing feature: for sample A the oscillation amplitude is strongly suppressed below about $T = 2 - 3\text{ K}$, Fig. 2(a). In contrast in sample B, Fig. 2(b), the canonical Lifshitz-Kosevich (LK) behavior is recovered. In the context of the Bloch-Grüneisen theory, suppression of SdH amplitude could be interpreted as originating from renormalization of the quasiparticle effective mass from the pure band mass m^* to an effective mass renormalized by the e-p interaction: $m^* = m_{\text{band}}(1 + \lambda)$, where λ is the e-p coupling constant [22,23]. Similar suppression of QO amplitude at low temperatures has been related in the past to highly unconventional physics, including mass divergence close to quantum criticality [24]. Comparison of the Fermi velocities of sample A (sample B of Ref. [13]) and the measured speed of longitudinal acoustic phonons (C_{11} mode) $v_a^L \approx 3375\text{ m/s}$, allows the estimation $\Theta_{BG} \approx 2.7\text{ K}$ —coinciding with the onset of the SdH oscillation amplitude suppression. However, the magnitude of the SdH amplitude suppression would suggest an effective mass increase by more than a factor of two. This would require a very strong e-p coupling, in contrast with previous estimates [13,25].

In order to address this apparent contradiction we have resorted to a different probe of the quasiparticle effective

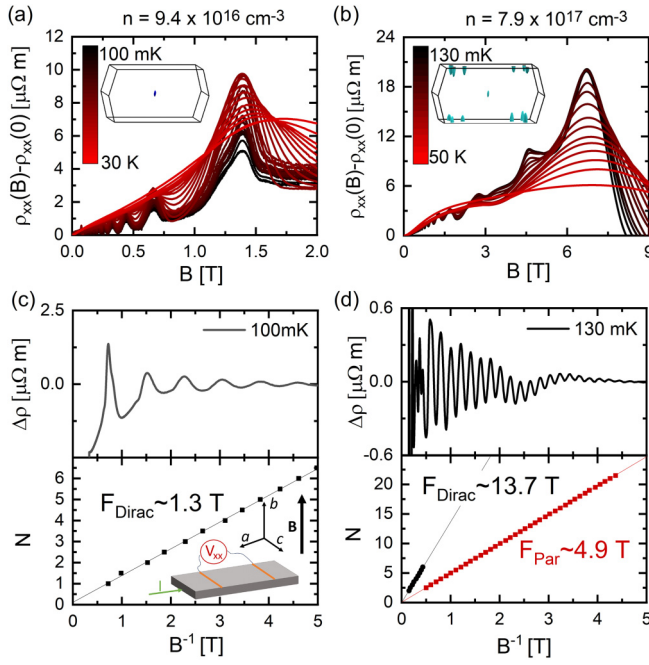


FIG. 1. Shubnikov-de Haas oscillations in ZrTe_5 in the sub-K range. (a) Magnetic-field dependence of the longitudinal electrical resistivity ρ_{xx} of sample A at various temperatures between 100 mK and 30 K with electrical current applied along the a axis of the crystals and magnetic field applied along b , inset shows calculated Fermi surface for the chemical potential crossing only the bottom of the Dirac band at Gamma. (b) Magnetic-field dependence of the longitudinal electrical resistivity ρ_{xx} of sample B at various temperatures between 130 mK and 50 K with electrical current applied along a and magnetic field applied along b , inset shows evolution Fermi surface of ZrTe_5 for higher charge carrier density samples. (c) SdH oscillations of sample A plotted vs inverse field together with the Landau fan diagram used for indexing the oscillations. Inset shows the measurement geometry with respect to the crystal axis. (d) SdH oscillations of sample B plotted vs inverse field together with the Landau fan diagram used for indexing the oscillations originating from different FS pockets.

mass. Although measurements of the SdH effect are the most widely used tool for the study of quantum oscillations in semimetals, their interpretation can in principle be much more difficult than other, thermodynamic, probes. The difficulty lies in the fact that magnetoresistance measurements are primarily a probe of momentum relaxation. Typically, in such measurements, one assumes that at low enough temperatures, momentum relaxation becomes temperature and field independent and thus the SdH oscillation amplitude reflects the field induced oscillations of the density of states and thus the effective mass [22]. This, however, does not necessarily have to be the case. Thus, to verify whether the suppression of QO in ZrTe_5 can be interpreted as an enhancement of the effective mass, we measured the temperature dependence of QO seen in the speed of sound. Velocity of sound is directly related to the system's elastic modulus and thus is a thermodynamic quantity that can be expected to directly reflect the field and temperature dependence of the free energy without spurious scattering effects [26,27].

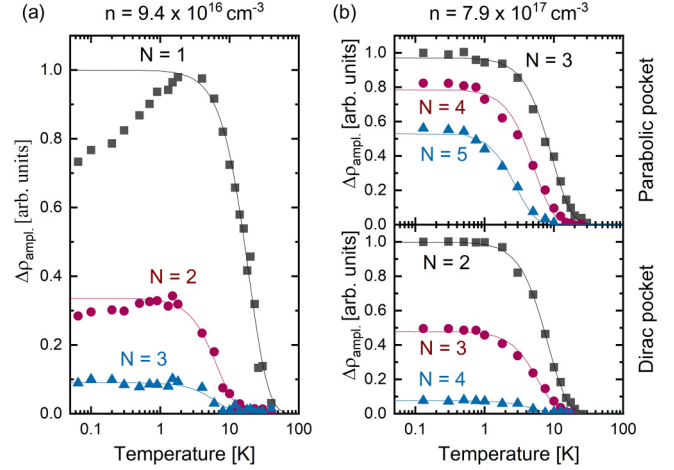


FIG. 2. Temperature dependence of SdH oscillations of samples A and B. (a) SdH amplitude as a function of T measured on sample A for three different magnetic fields. (b) SdH amplitude for both FS pockets as a function of T measured on sample B for three magnetic fields. The dots are experimental data. The lines are fits using the LK formula taking into account data from $T > 2$ K. N is the Landau level index in all panels.

Ultrasonic measurements require special sample surface preparation and thus we have selected an additional sample from the same growth batch as sample A in order to leave sample A intact for future measurements. Crucial aspect of the ultrasonic experiments was ensuring that the sample was not heated during the measurements at sub-kelvin temperatures. To ensure this we have used 1kHz pulse repetition rate with 400 ns pulse duration on a 2.73 mm long sample using the lowest possible transducer excitation. In addition the sample temperature was monitored using a Cernox thermometer located at the sample site.

Figure 3(a) shows the low temperature field dependence of the speed of sound of the C_{11} mode with magnetic field applied parallel to the b axis. Analysis of the frequency of magnetoacoustic oscillations measured in sample C reveals it enters the quantum limit at a similar field as sample A, confirming that both samples share similar charge carrier density. However, in contrast to the SdH oscillations seen in sample A, Fig. 3(b), the amplitude of the magnetoacoustic quantum oscillations in sample C does not reveal any amplitude suppression at low temperature. Instead, the oscillation amplitude saturates following the standard LK behavior, Fig. 3(c). The discrepancy in the behavior of the QO observed in thermodynamic and transport measurements suggests that the anomalous SdH amplitude originates from a low temperature change in the momentum relaxation of the electron fluid.

In the absence of a lattice, all electron-electron (e-e) collisions conserve momentum, in such circumstance there is no way for a single component electron fluid to dissipate its momentum. However, in the presence of the lattice, electrons can lose momentum via so-called Umklapp processes, where collisions can scatter electrons to a neighboring BZ, transferring a reciprocal lattice vector of momentum (G) to the lattice. Such processes, although very efficient in relaxing momentum, are only possible if the FS spans at least half of

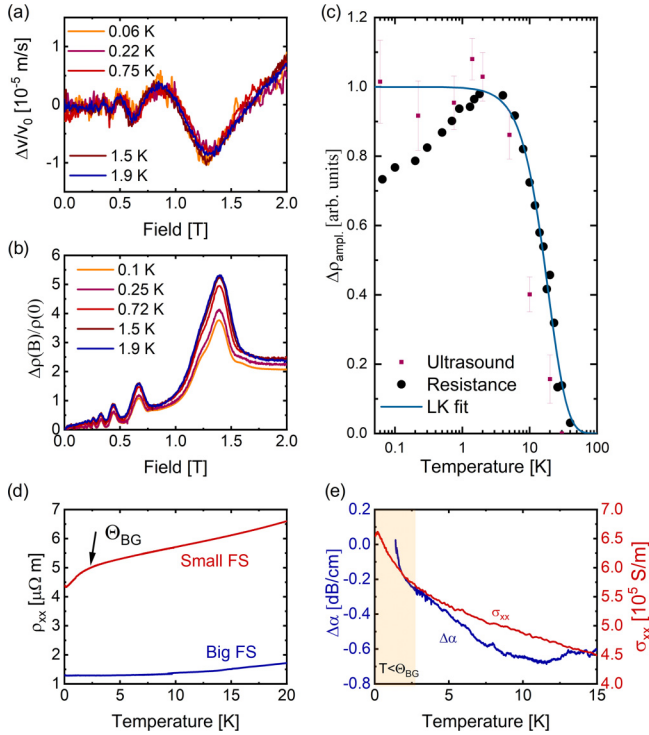


FIG. 3. Comparison of resistance measurements with sound propagation and attenuation measurements. (a) Magnetoacoustic quantum oscillations measured in sample C with a longitudinal sound mode propagating along the a axis and field applied along the b axis. (b) SdH effect measured in sample A [see also Fig. 1(a)]. (c) Comparison of QO amplitudes obtained from speed-of-sound and magnetoresistance measurements. (d) Comparison of zero-field resistances measured in samples A and B. Sample A with a small FS exhibits an anomalous downturn at low temperatures. The resistance in sample B, in contrast, saturates at low T . (e) Comparison of the zero-field electrical conductivity measured in sample A with the sound attenuation measured in sample C. Both quantities exhibit an anomalous increase on crossing Θ_{BG} with a stronger effect seen in the sound attenuation reflecting a rapid increase of the electron-liquid viscosity.

the BZ, and are strongly suppressed for smaller FSs [3] [4]. Thus, for small FSs such as those found in samples A and C where the FS comprises of less than 5% of the BZ [13], the main route for momentum relaxation, in the absence of disorder, is through electron-phonon (e-p) collisions where the electron liquid leaks momentum to the phonon gas. Consequently, the suppression of the SdH oscillations seems to emerge from suppression of e-p collisions below the BG temperature. This interpretation is corroborated by the absence of the SdH amplitude suppression in sample B that contains several FS sheets and where Umklapp processes are expected to play an important role in momentum dissipation even at low temperatures.

Additional evidence for the influence of Θ_{BG} on the low temperature properties of ZrTe_5 stems from the zero-field temperature dependence of resistivity. Figure 3(d) shows the temperature dependence of resistivity of samples A and B. In sample B, the low temperature resistance tends to saturate following the canonical behavior expected from the low

temperature resistance of metals $R(T) = R_0 + AT^2 + BT^5$ [1] with the quadratic term originating from e-e scattering events, the T^5 term from e-p scattering and R_0 being the residual resistivity due to impurities and imperfections [1]. In contrast, the resistance of sample A undergoes a highly anomalous transition with a rapid downturn on crossing Θ_{BG} . Before commenting further on this downturn, we describe an analogous anomaly in the sound attenuation.

The temperature dependence of sound attenuation is shown in sample C, see Fig. 3(e). Unlike sound velocity which is a thermodynamic probe, sound attenuation is a probe of energy transfer akin to thermal conductivity [28]. In our ultrasound experiments we used a 314 MHz excitation; this translates to a wavelength of ca. 10 μm , an order of magnitude higher than the electron mean free path estimated from the Drude formula at $T = 2$ K, $l_{mfp} \approx 1.5$ μm . In this limit the ultrasonic attenuation is proportional to the electronic liquid viscosity ν [6,27]. It can be seen from Fig. 3(e) that the measured attenuation exhibits a sudden increase on crossing Θ_{BG} . In contrast, attenuation measured on the high carrier density sample does not exhibit any kinks or anomalies (for details, see the Supplemental Material [21]). Interestingly, the increase of electron viscosity is much sharper than that seen in conductivity. An increase of electron viscosity is expected once e-p scattering is suppressed, however, Bloch-Gruneisen theory suggests that both conductivity and viscosity should follow a T^{-1} dependence at high temperatures and T^{-5} below Θ_{BG} [6]. Although in the present case at high temperatures the dependence is roughly linear, it decreases much faster than the predicted T^{-5} law at low temperatures. Notably, resistivity has the opposite curvature around Θ_{BG} to what is conventionally expected. Here we would like to highlight the robustness of the effect: the same effect is observed in two different Te-flux grown samples, using measurement methods based on distinctively different physical phenomena (conductivity and sound attenuation). In addition we have found a similar effect in CVT grown HfTe_5 samples with charge carrier densities similar to samples A and C (for details see the SM). Our experiments thus demonstrate that the observed effect is intrinsic and related to a low Θ_{BG} , small charge carrier density, and lack of Umklapp scattering processes. One obvious suspect in such conditions could be phonon drag. However, comparison of the measured data with a variational calculation of e-p scattering rates (see the SM for details) that take into account details of the Fermi surface geometry, phonon velocity anisotropies, and phonon drag excludes such an origin.

Recently, the low temperature resistivity of small Fermi surface metals has been discussed in the context of $\text{Bi}_2\text{O}_2\text{Se}$ and SrTiO_3 [3,29]. Here it was shown that resistance follows the canonical Fermi liquid predictions with $R(T) \approx T^2$ at low temperatures. Although the T^2 resistivity law is usually taken as a hallmark of Fermi liquid behavior, it is difficult to detect in common metals where resistance is dominated by the T^5 term originating from e-p processes [30], and as a consequence one observes a mixture of both behaviors prior to low temperature saturation. In the case of low-density metals, the increased e-e scattering cross section is expected to enhance the contribution of the T^2 term. However, for the T^2 term to be observable, there should be an additional process allowing the electron liquid to leak momentum (such

as multiple FS with mismatched effective masses or Umklapp processes) [16,30]. It has been argued that the electrical resistance of SrTiO₃ can instead be explained due to two-phonon scattering [31].

In our measurements we have not detected the T^2 resistance up to the lowest measured temperatures in low-density samples. Here we have focused on samples with a charge carrier density four times smaller than in previous experiments on Bi₂O₂Se and SrTiO₃ [3,29]. This, in combination with the small phonon velocity, conspires to place our samples into a very different regime. To our knowledge, this regime is the lowest observed Θ_{BG} allowing the study of transport across the Θ_{BG} , without the contribution of Umklapp processes and in the presence of Landau quantization.

Our experiments suggest a rapid increase of the electron fluid viscosity that could manifest an onset of a regime of viscous hydrodynamics. This could be qualitatively understood by comparing the frequency of momentum relaxing scattering with the quantum coherence time obtained from the field dependence of quantum oscillations [32]. The momentum relaxation scattering time can be estimated from the zero-field resistance using the Drude formula. At ≈ 2 K, using the parameters of sample A one obtains $\tau_e = 5.4$ ps. In contrast, the quantum coherence time previously extracted from the SdH effect on sample A (see sample B of Ref. [13]) at the same temperature, depending on the field orientation, is in the range 0.2–0.9 ps. This suggests that the dynamics of the electrons in ZrTe₅ at low temperatures has a strong contribution from normal e-e collisions with rare momentum relaxing collisions.

We have already seen that crossing Θ_{BG} and entering the regime of increased viscosity has a profound impact on the SdH oscillations. Indeed, comparison of the zero field resistance from Fig. 3(d), with the temperature dependence of the quantum oscillations amplitude in Fig. 1(a), reveals that the resistance at the maxima of the SdH oscillations is suppressed stronger than zero field resistance. This observation, together with the fact that the temperature dependence of quantum oscillation represents the Fourier transform of the electron distribution function in energy [33], could suggest that on cooling through Θ_{BG} , electrons decouple from the thermal bath and are able to remain in a nonequilibrium distribution. Such a scenario would be in qualitative agreement with SdH amplitudes deviating from the LK formula due to a continuous pumping of momentum to the electron liquid by the electric field and with thermodynamic magnetoacoustic oscillations exhibiting standard behavior. However, confirmation of this exciting possibility requires further theoretical work and experiments such as a direct measurement of the temperature difference between the electron liquid and the lattice as temperature changes across Θ_{BG} .

To date, electron hydrodynamics has been studied in several 3D compounds, notably WTe₂ [34], WP₂ [35,36], PdCoO₂ [32], and elemental antimony [4]. In these studies, signatures of hydrodynamic flow have been primarily inferred from the influence of boundary scattering on transport properties. However, to date, the temperature dependence of viscosity of the electron liquid on entering the hydrodynamic regime has not been directly probed. In the light of the anomalous response seen in both conductivity and

sound attenuation in our experiments we believe it is crucial to investigate sound attenuation in those compounds across different predicted regimes [37]. Here an interesting issue is that in most theoretical treatments of electron hydrodynamics and e-p coupling, it is assumed that the speed of sound is much smaller than the Fermi velocity and interactions are short range. This is contrary to the conditions found in ZrTe₅ since the ratio of the speed of sound and along the b axis obtained from inelastic x-ray scattering on ZrTe₅ (for details, see the SM) and the Fermi velocity is of the order of ~ 0.2 , and thus beyond usual assumptions. In addition, our estimate of the Thomas-Fermi screening length indicates that the screening length exceeds several unit cells and thus e-e interactions cannot be treated as strictly short ranged (for details, see the SM).

In summary, we have identified a possible onset of an electron hydrodynamic regime in the Dirac semimetal ZrTe₅. Our measurements suggest that reduction of e-p scattering below Θ_{BG} in the absence of Umklapp processes leads to an anomalous enhancement of electron viscosity and conductivity. In high magnetic fields, the interplay of the increased conductivity and presence of Landau quantization lead to an unconventional suppression of the amplitude of the Shubnikov-de Haas effect at low temperatures. Furthermore, we have demonstrated that the relevant temperature scales of the pentatellurides enable the study of a so far inaccessible regime where the presence of quantum oscillations overlaps with the hydrodynamic regime. In particular the possibility of easy exfoliation and production of field-gateable devices with submicron size makes ZrTe₅ an excellent testing platform allowing for excellent level of control of channel size and carrier concentration to study effects of electron viscosity [38].

O.K.F. acknowledges funding by the Swedish Research Council (VR) via a Grant No. 2022-06217 and the Foundation Blanceflor 2023 fellow scholarship. H.F.L. acknowledges funding by the Georg H. Endress foundation. T.M. acknowledges funding by the Deutsche Forschungsgemeinschaft (DFG) via the Emmy Noether Programme (Quantum Design Grant No. ME4844/1, Project ID 327807255), Project No. A04 of the Collaborative Research Center SFB 1143 (Project ID 247310070), the Cluster of Excellence on Complexity and Topology in Quantum Matter ct.qmat (EXC 2147, Project ID 390858490), as well as from the Luxembourg National Research Fund (FNR) and the DFG through the CORE grant “Topology in relativistic semimetals (TOPREL)” (FNR Project No. C20/MS/14764976 and DFG Project No. 452557895). Y.W. acknowledges funding support from the Chinese Academy of Sciences (Projects No. YSBR047 and No. E2K5071). We acknowledge the support of the Hochfeld-Magnetlabor Dresden (HLD) at HZDR, member of the European Magnetic Field Laboratory (EMFL), the DFG through the Collaborative Research Center SFB 1143 (Project No. 247310070), and the Wurzburg-Dresden Cluster of Excellence ct.qmat (EXC 2147, Project No. 39085490), S.G., J.G., B.V., D.H.N., and S.P. acknowledge funding by the European Union’s Horizon 2020 Research and Innovation Programme (Grant Agreement No. 824109, the European

MicroKelvin Platform); S.G., J.G., and C.F. by the DFG through the Forschergruppe FOR 5249 (QUAST); and D.H.N.

and S.P. by the Austria Science Fund (FWF) through I 5868-N (FOR 5249, QUAST).

- [1] J. M. Ziman, *Electrons and Phonons: The Theory of Transport Phenomena in Solids* (Oxford University Press, Oxford, 2001).
- [2] D. K. Efetov and P. Kim, Controlling electron-phonon interactions in graphene at ultrahigh carrier densities, *Phys. Rev. Lett.* **105**, 256805 (2010).
- [3] X. Lin, B. Fauqué, and K. Behnia, Scalable T^2 resistivity in a small single-component Fermi surface, *Science* **349**, 945 (2015).
- [4] A. Jaoui, B. Fauqué, and K. Behnia, Thermal resistivity and hydrodynamics of the degenerate electron fluid in antimony, *Nat. Commun.* **12**, 195 (2021).
- [5] S. A. Hartnoll and A. Mackenzie, *Colloquium: Planckian dissipation in metals*, *Rev. Mod. Phys.* **94**, 041002 (2022).
- [6] F. S. Khan and P. B. Allen, Sound attenuation by electrons in metals, *Phys. Rev. B* **35**, 1002 (1987).
- [7] C.-w. Cho, P. Wang, F. Tang, S. Park, M. He, R. Lortz, G. Gu, Q. Li, and L. Zhang, Thermal transport properties and some hydrodynamic-like behavior in three-dimensional topological semimetal ZrTe₅, *Phys. Rev. B* **105**, 085132 (2022).
- [8] W. Zhang, C. N. Kuo, S. T. Kuo, C. W. So, J. Xie, K. T. Lai, W. C. Yu, C. S. Lue, H. C. Po, and S. K. Goh, Tunable non-Lifshitz–Kosevich temperature dependence of Shubnikov–de Haas oscillation amplitudes in SmSb, *npj Quantum Mater.* **8**, 55 (2023).
- [9] F. Wu, C. Guo, M. Smidman, J. Zhang, Y. Chen, J. Singleton, and H. Yuan, Anomalous quantum oscillations and evidence for a non-trivial Berry phase in SmSb, *npj Quantum Mater.* **4**, 20 (2019).
- [10] J. Mutch, W.-C. Chen, P. Went, T. Qian, I. Z. Wilson, A. Andreev, C.-C. Chen, and J.-H. Chu, Evidence for a strain-tuned topological phase transition in ZrTe₅, *Sci. Adv.* **5**, eaav9771 (2019).
- [11] P. Zhang, R. Noguchi, K. Kuroda, C. Lin, K. Kawaguchi, K. Yaji, A. Harasawa, M. Lippmaa, S. Nie, H. Weng, V. Kandyba, A. Giampietri, A. Barinov, Q. Li, G. D. Gu, S. Shin, and T. Kondo, Observation and control of the weak topological insulator state in ZrTe₅, *Nat. Commun.* **12**, 406 (2021).
- [12] S. Galeski, H. F. Legg, R. Wawrzyńczak, T. Förster, S. Zherlitsyn, D. Gorbunov, M. Uhlarz, P. M. Lozano, Q. Li, G. D. Gu, C. Felser, J. Wosnitza, T. Meng, and J. Gooth, Signatures of a magnetic-field-induced Lifshitz transition in the ultra-quantum limit of the topological semimetal ZrTe₅, *Nat. Commun.* **13**, 7418 (2022).
- [13] S. Galeski, T. Ehmcke, R. Wawrzyńczak, P. M. Lozano, K. Cho, A. Sharma, S. Das, F. Küster, P. Sessi, M. Brando, R. Kuchler, A. Markou, M. König, P. Swekis, C. Felser, Y. Sassa, Q. Li, G. Gu, M. V. Zimmermann, O. Ivashko *et al.*, Origin of the quasi-quantized Hall effect in ZrTe₅, *Nat. Commun.* **12**, 3197 (2020).
- [14] F. J. DiSalvo, R. M. Fleming, and J. V. Waszczak, Possible phase transition in the quasi-one-dimensional materials ZrTe₅ or HfTe₅, *Phys. Rev. B* **24**, 2935 (1981).
- [15] S. Galeski, X. Zhao, R. Wawrzyńczak, T. Meng, T. Förster, P. M. Lozano, S. Honnali, N. Lamba, T. Ehmcke, A. Markou, Q. Li, G. Gu, W. Zhu, J. Wosnitza, C. Felser, G. F. Chen, and J. Gooth, Unconventional Hall response in the quantum limit of HfTe₅, *Nat. Commun.* **11**, 5926 (2021).
- [16] C. Wang, Thermodynamically induced transport anomaly in dilute metals ZrTe₅ and HfTe₅, *Phys. Rev. Lett.* **126**, 126601 (2021).
- [17] E. Skelton, T. Wieting, S. Wolf, W. Fuller, D. Gubser, T. Francavilla, and F. Levy, Giant resistivity and x-ray diffraction anomalies in low-dimensional ZrTe₅ and HfTe₅, *Solid State Commun.* **42**, 1 (1982).
- [18] Y. Zhang, C. Wang, G. Liu, A. Liang, L. Zhao, J. Huang, Q. Gao, B. Shen, J. Liu, C. Hu, W. Zhao, G. Chen, X. Jia, L. Yu, L. Zhao, S. He, F. Zhang, S. Zhang, F. Yang, Z. Wang *et al.*, Temperature-induced Lifshitz transition in topological insulator candidate HfTe₅, *Sci. Bull.* **62**, 950 (2017).
- [19] Y. Zhang, C. Wang, L. Yu, G. Liu, A. Liang, J. Huang, S. Nie, X. Sun, Y. Zhang, B. Shen *et al.*, Electronic evidence of temperature-induced Lifshitz transition and topological nature in ZrTe₅, *Nat. Commun.* **8**, 15512 (2017).
- [20] J. I. Facio, E. Nocerino, I. C. Fulga, R. Wawrzyńczak, J. Brown, G. Gu, Q. Li, M. Mansson, Y. Sassa, O. Ivashko, M. v. Zimmermann, F. Mende, J. Gooth, S. Galeski, J. van den Brink, and T. Meng, Engineering a pure Dirac regime in ZrTe₅, *SciPost Phys.* **14**, 066 (2023).
- [21] See Supplemental Material at <http://link.aps.org/supplemental/10.1103/PhysRevB.110.L121103> for additional data on ZrTe₅ and HfTe₅ samples, calculation of the Fermi screening length, discussion of the phon drag effect, details of charge carrier density and quantum oscillation amplitude extraction, experimental results on inelastic x-ray scattering, *ab initio* calculation of scattering lifetime, description of sample synthesis, and preparation methods, which includes Refs. [39–47].
- [22] D. Shoenberg, *Magnetic Oscillations in Metals* (Cambridge University Press, Cambridge, 1984).
- [23] P. Coleman, *Introduction to Many-Body Physics* (Cambridge University Press, Cambridge, 2015).
- [24] A. McCollam, S. R. Julian, P. M. C. Rourke, D. Aoki, and J. Flouquet, Anomalous de Haas-van Alphen oscillations in CeCoIn₅, *Phys. Rev. Lett.* **94**, 186401 (2005).
- [25] T. Ehmcke, S. Galeski, D. Gorbunov, S. Zherlitsyn, J. Wosnitza, J. Gooth, and T. Meng, Propagation of longitudinal acoustic phonons in ZrTe₅ exposed to a quantizing magnetic field, *Phys. Rev. B* **104**, 245117 (2021).
- [26] D. LeBoeuf, C. Rischau, G. Seyfarth, R. Kuchler, M. Berben, S. Wiedmann, W. Tabis, M. Frachet, K. Behnia, and B. Fauqué, Thermodynamic signatures of the field-induced states of graphite, *Nat. Commun.* **8**, 1337 (2017).
- [27] B. Luthi, *Physical Acoustics in the Solid State* (Springer, Berlin, 2005).
- [28] M. Holland, Thermal conductivity and ultrasonic attenuation, *IEEE Trans. Sonics Ultrason.* **15**, 18 (1968).
- [29] J. Wang, J. Wu, T. Wang, Z. Xu, J. Wu, W. Hu, Z. Ren, S. Liu, K. Behnia, and X. Lin, T -square resistivity without Umklapp

- scattering in dilute metallic $\text{Bi}_2\text{O}_2\text{Se}$, *Nat. Commun.* **11**, 3846 (2020).
- [30] K. Behnia, On the origin and the amplitude of T -square resistivity in Fermi liquids, *Annalen der Physik* **534**, 2100588 (2022).
- [31] A. Kumar and V. Y. and D. L. Maslov, Quasiparticle and non-quasiparticle transport in doped quantum paraelectrics, *Phys. Rev. Lett.* **126**, 076601 (2021).
- [32] P. J. W. Moll, P. Kushwaha, N. Nandi, B. Schmidt, and A. P. Mackenzie, Evidence for hydrodynamic electron flow in PdCoO_2 , *Science* **351**, 1061 (2016).
- [33] S. Sebastian and C. Proust, Quantum oscillations in hole-doped cuprates, *Annu. Rev. Condens. Matter Phys.* **6**, 411 (2015).
- [34] U. Wool, A. Hamo, G. Varnavides, Y. Wang, T. X. Zhou, N. Kumar, Y. Dovzhenko, Z. Qiu, C. A. C. Garcia, A. T. Pierce, J. Gooth, P. Anikeeva, C. Felser, P. Narang, and A. Yacoby, Imaging phonon-mediated hydrodynamic flow in WTe_2 , *Nat. Phys.* **17**, 1216 (2021).
- [35] J. Gooth, F. Menges, N. Kumar, V. Suss, C. Shekhar, Y. Sun, U. Drechsler, Zierold, C. Felser, and B. Gotsmann, Thermal and electrical signatures of a hydrodynamic electron fluid in tungsten diphosphide, *Nat. Commun.* **9**, 4093 (2018).
- [36] J. Coulter, R. Sundararaman, and P. Narang., Microscopic origins of hydrodynamic transport in the type-II Weyl semimetal WP_2 , *Phys. Rev. B* **98**, 115130 (2018).
- [37] X. Huang and A. Lucas, Electron-phonon hydrodynamics, *Phys. Rev. B* **103**, 155128 (2021).
- [38] Y. Liu, H. Pi, K. Watanabe, T. Taniguchi, G. Gu, Q. Li, H. Weng, Q. Wu, Y. Li, and Y. Xu, Gate-tunable multiband transport in ZrTe_5 thin devices, *Nano Lett.* **23**, 5334 (2023).
- [39] A. M. Brown, R. Sundararaman, P. Narang, W. A. Goddard, and H. A. Atwater, Nonradiative plasmon decay and hot carrier dynamics: Effects of phonons, surfaces, and geometry, *ACS Nano* **10**, 957 (2016).
- [40] C. J. Ciccarino, T. Christensen, R. Sundararaman, and P. N. and, Dynamics and spin-valley locking effects in monolayer transition metal dichalcogenides, *Nano Lett.* **18**, 5709 (2018).
- [41] D. R. Hamann, Optimized norm-conserving Vanderbilt pseudopotentials, *Phys. Rev. B* **88**, 085117 (2013).
- [42] N. Aryal, X. Jin, Q. Li, A. T. A, and W. Yin, Topological phase transition and phonon-space Dirac topology surfaces in ZrTe_5 , *Phys. Rev. Lett.* **126**, 016401 (2021).
- [43] A. Garcia, J. Coulter, and P. Narang, Optoelectronic response of the type-I Weyl semimetals TaAs and NbAs from first principles, *Phys. Rev. Res.* **2**, 013073 (2020).
- [44] S. Abedi, S. Vitkalov, and N. Mikhailov, Anomalous decay of quantum resistance oscillations of 2D helical electrons in magnetic field, *Sci. Rep.* **10**, 7875 (2020).
- [45] R. Sundararaman, K. Letchworth-Weaver, K. A. Schwarz, D. Gunceler, Y. Ozhabes, and T. Arias, JDFTx: Software for joint density-functional theory, *SoftwareX* **6**, 278 (2017).
- [46] R. T. Azuah, L. Kneller, Y. Qiu, P. Tregenna-Piggott, C. Brown, J. Copley, and R. Dimeo, Dave: A comprehensive software suite for the reduction, visualization, and analysis of low energy neutron spectroscopic data, *J. Res. Natl. Inst. Stand. Technol.* **114**, 341 (2009).
- [47] P. Böttcher, Tellurium-rich tellurides, *Angew. Chem. Int. Ed. Engl.* **27**, 759 (1988).